Tubular Anodes with Hidden Catalyst Concept and their Hydrogen Transport

Luis Bambace[1], Alfredo Castro[2] , Renata Favalli[2], Fernando Ramos[1], Hélcio Villanova[1]

[1] National Institute for Space research INPE, São José dos Campos, BR, Tel: 55-12-3945-6154, Fax: 55-12-3945-6163, Email: bambace@dem.inpe.br
[2] Nuclear and Energetics Research Institute IPEN, São Paulo, BR Tel: 55-11-3133-9452, Fax: 55-12-3945-6163, Email: ajcastro@ipen.br

1 Introduction

This paper discusses the operation of patent pending fuel cell anodes made with microfiber fabrics as templates for tubular structures of porous walls with less than 1 μm compact outer layer, and external diameter under 20 μm. These anodes are able to operate with Hydrogen of relatively high CO content. Metal nm texture foam walls or entangled carbon nanotubes (nm-tubes) walls are filled with ionomer. A 18 nm thickness low porosity nickel shell over tubes was made, due to a proper activation with very close nm catalyst particles and chlorides accelerators impregnation of the ionomer. Accelerator use assures a growing rate parallel to ionomer surface higher than in other directions. Niobium or Vanadium shells may be pulsed electroplated temperatures in the 29-110 °C range with non aqueous ionic liquids. Palladium deposition is also possible. the minimum thickness of low porosity shells is higher for all other metals as any accelerator was used, but still bellow 1.5 times the foam cell size thanks to the distribution of catalyst grains.

2 Material and Methods

Using either polymer, copper or alumina μm-fiber fabrics as removable templates, and either pulsed electroplating or chemical vapor deposition techniques, porous wall tubes of internal and external diameters in the ranges of 6-12 μm and 10-16 μm, respectively, were made. The structures were filled with ionomer, catalyst and finally received a hydrogen (H) permeable shell layer. Some material are known to have low electrical resistance and good hydrogen transport properties, such as solubility and diffusion. Particularly, the permeability, the product of solubility by the diffusion coefficient is the crucial property to the determination of H transport through a shell. Niobium (Nb), Vanadium (V) and Tantalum (Ta) have not only the highest hydrogen permeability, but also permeabilities that increase the colder is the environment. Palladium (Pd) permeability is just below these materials, but with values that increase with temperatures. Iron (Fe) and nickel (Ni) come next, with similar behavior. Exact values of permeability of these last two metal depend on the type crystal structure and also of grain size, as interstitial transport is much higher than by the grain body one. Metals H content, in general, are proportional to the square root of pressure, while some polymers H content is proportional to pressure. Carbon is not amongst the best H_2 permeable material, but as carbon nm-tubes have very thin walls, and as they are hollow their H_2 transport were evaluated. The main sources of permeability data are references [1] to [8]. The most important data for 1 atm H_2 pressure and operation between 60 and 120°C are in table 1 and 2.

To calculate the H and CO fluxes it is necessary to use some "flux resistances" in analogy with thermal or real electric resistances. The first one is the H transport resistance by diffusion in the shell, R_{SH}, associated with inner, R_{OH}, and outer, R_{IH}, interface resistances, related to release and capture oh H_2 by the surfaces. Due to the low dependence of thermal contact resistance with thickness, a constriction resistance $R_{CONST-H}$, equal to half of the contact resistance of Cooper [9] model, describes additional difficulties to H flux toward catalyst grains. It is assumed that H_2 adsorbed at a cylindrical surface, goes to an spherical particle, with half of it in the ionomer and half of it in the metal wall, and a internal catalyst particle resistance R_{CIH} is put in series with the two. There are pores in the shell, as due to random catalyst particles positions and random aspects of structure and its small size neither an integer number of atoms fits in the space, nor it is possible to overcome differences by structural deformation in all cases. The number of pores is bigger than the number of activating particles, and there are some very small pores directly on the particles, as the interatomic distances of different materials does not match. So, many pores in parallel carry either H_2 or CO to the ionomer, with resistances R_{PI-CO} and R_{PI-H}, and resistances related to access of gases trough pores to the catalyst particles, R_{PC-CO} and R_{PC-H} are linked to the single to multiple spots coplanar coupling in semi-infinite media. R_{ICH} and R_{ICCO} are internal resistances of particle to gases coming from these pores to the catalyst-ionomer interfaces A Cooper constriction resistance $R_{CONST-O}$ shall be added to O_2. Resistances R_{PI-X} are far bigger than diffusion ones in gas or liquid filled pores cases with diameters smaller than 1 nm. In gas filled case, the Knudsen number based in diameters are very big, and they behave alike a vacuum system pipe,

with a conductance equal the surface diffusion one in parallel with another obtained with the sum of probabilities of a molecule to pass directly, plus the ones of passing hitting the wall with a given specular and diffuse reflections chances, translated by the accommodation coefficient. If filled with liquid the pores will have a boundary layer of adsorbed molecules and organized molecules attracted by their dipoles that blocks the flux of CO and H_2, so pore effective diameter, d_{PE} is reduced by twice this layer thickness.

$$R_{SH} = (2\,\pi\,L\,p_{HS})^{-1}\,\ln(d_{SHE}/d_{SHI}) \quad (1)$$

$$R_{CONST\text{-}X} = 0.25\,\pi^{-1}\,a^{-1}\,(1\text{-}a/b)^{3/2}/n \quad (2)$$

$$R_{X\text{-}IE} = f_I\,(2\,\pi\,L\,\tau_I\,p_{XI})^{-1}\,\ln(d_{SHI}/d_{TI}) \quad (3)$$

$$R_{PC\text{-}X} \sim [\Sigma\, 0{,}5^{0,5}(d_{PE}^{-1}+b)+d_{ij}^{-1}]/\,p_{XI} \quad (4)$$

where p_{HS} is the H permeability of the shell, p_{XI} is the ionomer permeability to the gas X, τ_I is its tortuosity due to presence of the tube porous wall, f_I is the occupation factor of ionomer in the wall, the tube inner, inner shell and outer shell diameters are respectively d_{TI}, d_{SHI} and d_{SHE}; a is ¼ of the average area of a catalyst particle, b is $(4\,S\,n^{-1}\pi^{-1})^{1/2}$, for n the number of particles and S the area, d_{ij} are distances from source i to pore j. $R_{PC\text{-}X}$ is always bigger than real ones if all $d_{ij}\equiv 0$ Permeabilities are effective ones, due to the very small thickness of the system components, see [10].

Gases that reach the ionomer have a resistance related with its path toward inner electrolyte, $R_{H\text{-}IE}$ and $R_{CO\text{-}IE}$ and $R_{O\text{-}IE}$ to O_2 outward path. If the porous wall support material is a good H transport media, catalyst may be placed on it, and as its H transport is relevant the corresponding structure may be represented as a fin, with a length bigger than wall thickness to catch the effect of the tortuous path. In all cases some core to surface H_2 flux resistance is assumed. Due to an intrinsic porosity macromolecules have a bigger diffusion coefficient than a low permeability metal, and double fin model tested for the metal ionomer H_2 transfer and its end transfer to the electrolyte. So:

$$d^2C_i/dx^2 - b_{ii}C_i + b_{ij}C_j = 0 \quad (5)$$

C_1 and C_2 are base material and ionomer concentrations, $b_{12}=2h/(r_f D_1)$, in which h is the interface transfer coefficient r_f the equivalent foam/nm-tube fin radius, D_1 the diffusion coefficient; $b_{22}=b_{21}=2h/(r_{io}\,D_2)$, to D_2 the ionomer diffusion coefficient for r_{IO} the equivalent ionomer fin radius; $b_{11}=b_{12}-2i_o\cdot 10^{dec}/(r_f D_1)$ to i_o the exchange current, dec the number of decades of polarization. A bi-quadratic equation gives the exponential ratios. Boundary conditions are insulated tips at liquid and shell interfaces for metal/foam and ionomer fins, knew concentration at shell for both fins. By solving this with actual coupling b_{ij}, ones sees that the wall support material and ionomer are in equilibrium in short distances from the shell, so a single material model with average properties and eventual reaction used. This gives either a logarithmic field or a I_o Bessel function one, where the distance multiplied by $[4f i_o\cdot 10^{dec}/(r_f D_1)]^{0,5}$ is the argument, with f the support material volume fraction. Large argument approximations to I_v ,field / $R_{X\text{-}IE}$, $I_v(x)=e^x(2\pi x)^{-0,5}\{1-(4v^2-1)/(8x)+(4v^2-9)(4v^2-1)/(8x)^2\}$, is used in general. Due to the presence of internal liquid electrolyte and the small thickness of ionomer tubular layer, it will be assumed its pores are entirely filled with liquid electrolyte. The carbon nm-tubes typically have 16 nm, and 3 nm wall thickness, so mean free paths are respectively 10 and 6,6 nm to H_2 and CO. The Knudsen number is nearly one to H_2/H and near 2/3 to CO, surface diffusion is enhanced by free H/H_2 that jumps directly to distant points , and vacuum pipe calculation are valid. The resistances are combined according to the circuit shown in figure 1. The CO may be oxidized in the catalyst either reacting with water or with O_2, H_2O_2 or O_2H^+. The Pt catalyst H_2 and CO adsorption kinetic constants are $3.26\cdot 10^{-5}$ and, $3.26\cdot 10^{-5}$ m/s, desorption constants for H and CO are $3.81\cdot 10^{-6}$ and $2.74\cdot 10^{-11}$ mol $m^{-1}s^{-1}$, H and CO-OH_{ADS} exchange currents respectively 8 A/m^2 and $1.04\cdot 10^{-6}$ A/m^2. CO-O_2 exchange current is near 2.5 times CO-OH_{ADS} one, and H_2O_2-CO even higher. Sieverts ideal solid or Rault models solution kinetics are fast enough to equilibrium concentrations only to be considered. If excess ionomer is used, a internal pure layer of it brings an additional logarithmic resistance R_{OLX}.

Figure 1: Resistances in the Transport Model.

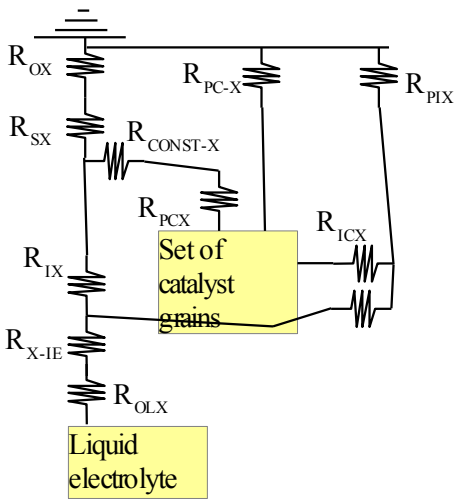

With this, the tolerance of the new architecture to high levels of CO in the fuel is evaluated as well as the cross flow of gases. Interface area for a given electrode thickness t_e and mean area diameter d_t, and tube fraction f_t in the electrode is $4f_t(t_e/d_t)$. But as a point approaches the electric insulator it has more react-

ivity, an efficiency factor α shall be used and effective area is $4\alpha f_t(t_e/d_t)$. For common PEM cells, there are only small differences in CO and H transfer coefficient to the catalyst, due mainly to different permeability of them in the liquid present in the electrode. As the ratio between the transfer coefficients of H and CO becomes bigger, the cell is less sensitive to CO. Another point in CO tolerance is its consumption, linked to water gas shift in anode, electrochemical oxidation, O_2 bleeding and eventual H_2O_2 presence. If the shell blocks O_2 its bleeding is safer, and despite of cathode consumption electrokinetic flows and small ionomer thickness allows some supply of O_2 to CO oxidation.

3 Results

The high hydrogen-cover shell interface area and the H transport at 80°C trough the shell assures its high concentration at catalyst for Pd, V and Nb shells. Ni shell case is uncertain due to a large variation of literature permeability data, probably related with the higher grain interfacing values. Either in cubic or in hexagonal compact crystals, interstitial H_2/H occurs, but the gaps are very close to H atomic diameter. Diffusion along grain boundaries seems to be the main mode, despite of vacancy, iterstitialcy and crowd-ion mechanisms. CO nickel transport papers confirms that hypothesis. Due to the dense nucleation of the catalyst grains, and auto-catalytic processes employed the system grain size, g_s, is from 1.6 to 3 nm, much smaller than any literature measured Ni sample as in [1], and the system operates at higher temperature. Using these results with typical Arrhenius temperature and grain size corrections, a permeability of $3.9 \cdot 10^{-10}$ is found. As the available grain contour perimeter per unit of area is proportional to $1/g_s$ permeabilities for our system are higher. Table 1 gives the equivalent partial H_2 pressure the catalyst grains should be exposed in gas environment to produce a flux of H_2 equivalent to the one assured by the set up at operational conditions, to catalyst loads of 0.1 mg-Pt/cm^2-bp or 0.05 mg-Pd/cm^2-bp, where the bp indicates that bipolar plate area is the reference. It was noticed that even with very small HER activity porous wall material, with an exchange current, i_f, of the order of 10^{-6}A/m^2, due to the large area and low electrode internal electrical resistance, almost no H_2 reaches internal electrolyte at 2 decades of chemical polarization for Ni foam setup despite the 2 to 3 μm ionomer thickness. This is easily shown with the ratio of $I_1(mx)$ fluxes at the 2 shell positions, calculated with large argument approximations. For carbon nanotube with diffusive approximation and V foam i_f must raise to $5 \cdot 10$-4A/m^2, and is near 8×10^{-5}A/m^2 for effective transition regime Monte Carlo analysis. The H content in feed gas may be reduced if the power is smaller. The shell pores are tiny in its inner, and eventually larger at outer layers if the shell is thick enough to defects propagation, or over 15 nm. Minimum low porosity shell thickness are about 16 nm to Ni (electroless), 60 nm to Pd, and 160 to ionic liquids electroplated V. As V is a very good H conductor its thickness was above minimum value. Thick shells of high H permeability material, blocks more effectively O_2 and CO, this made the natural O_2 bleeding to anode catalyst of the system, to be effectively blocked by the shell, so the feeding H_2 will not mix with O_2. As O_2 access to catalyst is partially blocked by the ionomer and even by liquid electrolyte, despite of its convective flow, levels are not harmful to catalysis, even CO content in feeding mixture is low, and its bleeding high enough to a fast oxidation of residual CO from dirty mixtures. In the case of 0.35 mm thick anodes, the Ni shell couplings for H_2, CO and O_2 are 0.328, 2.72E-2 and 4.09E-4 mol/m^2-bp/s/atm$^{0.5}$. This means a strong selectivity in favor to H_2. Palladium shell has an H_2 coupling of 6.9100 mol/m^2-bp/s/atm$^{0.5}$. Being thicker CO and O_2 couplings falls to 9E-3 and 1.4E-4 mol/m^2-bp/s/atm^{05}. The V shell couplings are 1.88E+8, 3.3E-3 and 4.9E-5 mol/m^2-bp/s/atm$^{0.5}$.for H_2, CO and O_2 respectively. This means that CO and O_2 transfer to H_2 feeding cavity is effectively blocked by the shell. Once the cell is off, H_2 blocking due to reaction ceases and filled Ni foam coupling becomes 0.16 mol/m2-bp/s/atm$^{0.5}$ only, critical for high permeability shells, being it necessary to cut H_2 feeding as soon as possible. Corresponding couplings to carbon nm-tubes and vanadium foam are even higher. CO and O_2 couplings are in the 8E-5 to 1.2 E-4 mol/m2-bp/s/atm$^{0.5}$ range. At operation the cell has an eletrokinetic convention and levels of O_2 about 0.04 mol/m^3 at liquid electrolyte so some residual O_2 will be available to help CO oxidation, and this kinetic is known to be better than adsorbed OH one.

Table 1: H_2 equivalent contents at catalyst for different shell materials $H_{2FLUX}=K(P_E^{0.5}-P_C^{0.5})$

Shell material & thickness (nm)	Current (A/m^2)	Sieverts H_2 Pressure loss (Pa)	Electrode thickness (mm)
Ni / 18	18500	50,000	0.35
Ni / 18	50000	95000	0.35
Pd /48	5000	0.2	0.35
Pd / 48	9000	0.4	0.35
V / 300	9000	5E-4	0.35

The average chemical polarization needed to produce the above currents, is very low, once the catalyst is plenty of H_2. In the 50000 A/m^2 Ni shell case, the concentration is equal pure water interface one to a pressure of 1.86 atm. Notice that more than half of the total catalysts grains area is operating in contact with

ionomer. Reported exchange currents for Pt in water with this equilibrium H_2 content is 8 A/m^2-Pt$_{EXPOSED}$. The current IPEN Pt or Pt-Ru grains diameter, produced by electron beam or radiation reduction in alcohol, is 1.5 nm, so for 50% of the grain inserted in the shell the catalysis area is 93 m^2. This means less 1.7 decades of polarization to reach 70000A/m^2-bp, or less as more than half of grain area is exposed to ionomer, notice that these grains are the seeds of autocatalytic process. Depending of reaction mechanism 100 to 120 mV. For other shells polarization is much smaller. Ionomer resistance is only 750 μΩcm/cm^2-bp for an anode with 16 μm external diameter tubes and a interface area to bipolar area ratio of 20 filled with Nafion. Even considering current distribution related losses are of few mV. This is the main reason less conductive ionomer may be used. An electronic microscope image of one of the tested structures is shown in figure 2. A complete cell setup is in figure 3. This tube has 10 μm of internal diameter, and it is not filled with ionomer to easy the image obtaining.

Figure 2: Complete cell setup

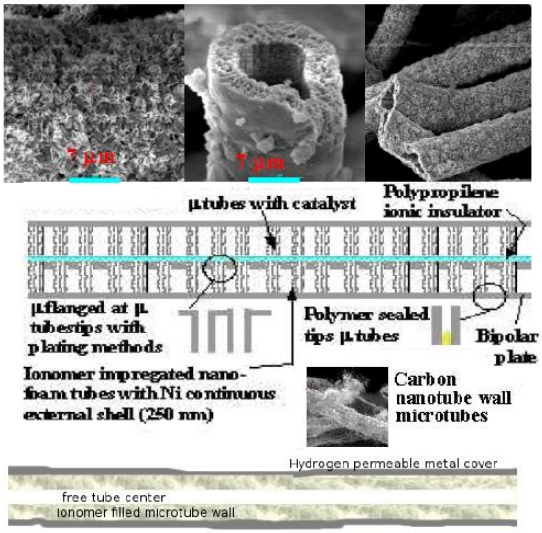

Figure 3. Typical 5 μm radius of anode fabrics.

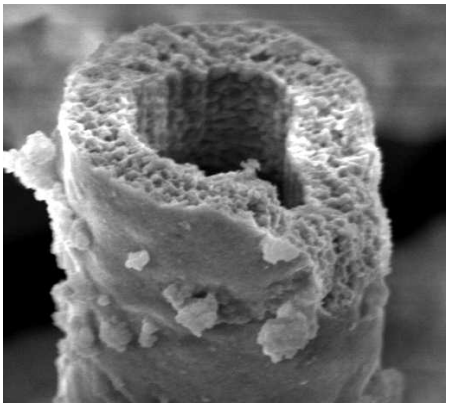

Ni foam has some catalytic activity, but as it is protected against corrosion in acid media with passivation layers of Ni-Cr-N, borides or oxides, with this protection it probably will not have any catalytic activity. Hence a small cost low activity catalyst is employed to avoid H_2 cross flow. The closer the catalyst is from outer wall, the more H_2 is available and the more efficient its use, this way top catalyst will be placed out of the wall only if there is not enough space on wall inner surface. Possible control catalysts are either organometallic or Ru-sulfides HER catalysts, used not with the purpose of current production but to block H_2 flow towards electrolyte, and to mitigate excessive O_2 transport. Arrangements with good H_2 penetration, as vanadium foam, offers more catalyst support area, but they have more cross flow problems. This foam showed over 20 times more H transport capacity than carbon nanotubes, due to the strong wall iteration of the latter. This and other tested geometries are the result of new nanotechnology and electrochemical processes in fuel cell design [11].

4 Conclusions

This study shows that tubular fabric anode systems with proper design are promising anodes for future high power fuels cells. Vanadium and Palladium shells allow proper H_2 flux, while effectively blocking CO and O_2. On the other hand with nickel it is not possible to assure a high enough hydrogen flux without further tests. How the permeability varies with the grain size reduction remains an open question. As the shell blocks the O_2 flux to fuel supply cavity, the small flux of O_2 in the ionomer helps the oxidation of any CO passing trough the shell. When the cell is operating at full power, H_2 that does not reacts in the main catalyst layer is oxidized in the porous wall matrix filled with ionomer. When the cell is H_2 crossing is about 0.16 mol/m^2-bp/s, implying in the need of immediate cut of its supply.

References

[1] Doylei, D. M; Palumbo, G; Aust K. T; El-Sherik A. M; ERB U. *Acta metall, mater:* Vol. 43, No. 8, pp. 3027 3033, 1995.

[2] Zajec,B; Nemanic,V. Determination of parameters in surface limited hydrogen permeation through metal membrane. Journal of Membrane Science 280 (2006) 335–342.

[3] Akamatsua,T; Kumea,Y; Komiyaa, K; Yukawaa, H; Morinagaa, M; Yamaguchib, S. Electrochemical method for measuring hydrogen permeability

through metals. *Journal of Alloys and Compounds* 393 (2005) 302–306.

[4] Kazarinov, R.F. Thin-film, Solid-state Proton Exchange Membranes for Fuel Cells. *Bell Labs*. 2005.

[5] Kocha,S.S; Yang, J.D; Yi, J.S. Characterization of Gas Crossover and Its Implications in PEM Fuel Cells. UTC Fuel Cells, South Windsor, CT 06074. DOI 10.1002/aic.10780. *Published online February 9, 2006 in Wiley InterScience*

[6] Choi, P. Investigation of Thermodynamic and Transport Properties of Proton-Exchange Membranes in Fuel Cell Applications. *Worcester Polytechnic Institute. PhD Thesis*. 2004.

[7] Sedano,L.A; Alberici, S; Perujo,A; Camposilvan, J; Douglas, K. Derivation of hydrogen transport parameters in carbon fibre composites by modelling transient release in isovolumetric desorption experiments. *Journal of Nuclear Materials* 258-263 (1998).

[8] Edwards, A. G. Measurement of the diffusion rate of hydrogen in nickel. *British Journal of Applied Physics* 406 (8), 1957

[9] Cooper, M. G., Mikic, B. B; Yovanovich, M. M., Thermal Contact Conductance. *Journal of Heat Mass Transfer*, 12, 279-300, 1969.

[10] Bitter, J.G.A. Transport Mechanisms in Membrane Separation Processes. Plenum Publishing Corporation. NY.ISBN 0-306-43849-6

[11] Galinski, M; Lewandowski, A; Stepniak, I. Ionic liquids as electrolytes. Electrochimica Acta 51, 5567-5580, 2006.